Proc. Natl. Acad. Sci. USA
Vol. 95, pp. 14045–14050, November 1998
Biochemistry

Structural basis for efficient phosphorylation of 3′-azidothymidine monophosphate by *Escherichia coli* thymidylate kinase

ARNON LAVIE*, NILS OSTERMANN*†, RALF BRUNDIERS†‡, ROGER S. GOODY*, JOCHEN REINSTEIN*, MANFRED KONRAD‡, AND ILME SCHLICHTING*§

*Department of Physical Biochemistry, Max Planck Institute for Molecular Physiology, Rheinlanddamm 201, 44139 Dortmund, Germany; and ‡Department of Molecular Genetics, Max Planck Institute for Biophysical Chemistry, 37018 Göttingen, Germany

Edited by Perry A. Frey, University of Wisconsin, Madison, WI, and approved September 11, 1998 (received for review June 29, 1998)

ABSTRACT **The crystal structures of *Escherichia coli* thymidylate kinase (TmpK) in complex with P^1-(5′-adenosyl)-P^5-(5′-thymidyl)pentaphosphate and P^1-(5′-adenosyl)P^5-[5′-(3′-azido-3′-deoxythymidine)] pentaphosphate have been solved to 2.0-Å and 2.2-Å resolution, respectively. The overall structure of the bacterial TmpK is very similar to that of yeast TmpK. In contrast to the human and yeast TmpKs, which phosphorylate 3′-azido-3′-deoxythymidine 5′-monophosphate (AZT-MP) at a 200-fold reduced turnover number (k_{cat}) in comparison to the physiological substrate dTMP, reduction of k_{cat} is only 2-fold for the bacterial enzyme. The different kinetic properties toward AZT-MP between the eukaryotic TmpKs and *E. coli* TmpK can be rationalized by the different ways in which these enzymes stabilize the presumed transition state and the different manner in which a carboxylic acid side chain in the P loop interacts with the deoxyribose of the monophosphate. Yeast TmpK interacts with the 3′-hydroxyl of dTMP through Asp-14 of the P loop in a bidentate manner: binding of AZT-MP results in a shift of the P loop to accommodate the larger substituent. In *E. coli* TmpK, the corresponding residue is Glu-12, and it interacts in a side-on fashion with the 3′-hydroxyl of dTMP. This different mode of interaction between the P loop carboxylic acid with the 3′ substituent of the monophosphate deoxyribose allows the accommodation of an azido group in the case of the *E. coli* enzyme without significant P loop movement. In addition, although the yeast enzyme uses Arg-15 (a glycine in *E. coli*) to stabilize the transition state, *E. coli* seems to use Arg-153 from a region termed Lid instead. Thus, the binding of AZT-MP to the yeast TmpK results in the shift of a catalytic residue, which is not the case for the bacterial kinase.**

Phosphorylation of AZT-MP by thymidylate kinase (TmpK; EC 2.7.4.9, ATP:dTMP phosphotransferase) has been implicated as the rate-limiting step in the activation pathway of the anti-HIV prodrug 3′-azido-3′-deoxythymidine (AZT). AZT must be phosphorylated by cellular enzymes to azidothymidine triphosphate before it can exert its antiviral effect by inhibiting HIV reverse transcriptase and acting as a chain terminator of nascent DNA strands. The bottleneck of AZT activation lies in the second phosphorylation step, the step that adds a phosphate group to azidothymidine monophosphate (AZT-MP) to yield azidothymidine diphosphate and is catalyzed by TmpK. Cells treated with AZT accumulate the toxic AZT-MP (1–3) in millimolar concentration (4, 5), and thus the active AZT triphosphorylated metabolite is at very low concentration. This situation is only slightly improved upon coinfection with herpes simplex virus I thymidine kinase-carrying vectors that efficiently phosphorylate the antiviral drugs acyclovir or ganciclovir but not AZT or AZT-MP (6, 7).

Therefore, we set out to understand the structural basis for the slow activation of AZT-MP. The structures of the yeast TmpK ($TmpK_{yeast}$) complexed with either the physiological substrate dTMP or the partially activated prodrug AZT-MP indicate that it is the interaction of the 3′-deoxyribose substituent with a carboxylic acid side chain located in the P loop sequence that is responsible for the reduced rate with AZT-MP (8, 9). This interaction causes a P loop movement to accommodate the bulky and rigid azido group of AZT-MP. The residue after this carboxylic acid is Arg-15 and it was shown to play a catalytic role (10). Thus, we postulated that it is the resulting arginine displacement that is responsible for the reduced phosphorylation rate. Our interest in TmpK from *Escherichia coli* ($TmpK_{coli}$) arose when we realized that it lacks this catalytic arginine in the P loop (having a glycine instead) although the P loop carboxylic acid is retained, albeit as glutamic acid in contrast to the aspartic acid in the yeast enzyme. This led to the hypothesis that even if a similar P loop shift were to occur upon AZT-MP binding to $TmpK_{coli}$, it should not have such a drastic effect on catalysis (10). Kinetic measurements support our hypothesis, showing that the rate of AZT-MP phosphorylation at saturating substrate concentrations is reduced by only a factor of 2 in comparison to dTMP, whereas this factor is 200 for the $TmpK_{yeast}$ (10). The crystal structures of $TmpK_{coli}$ complexed with P^1-(5′-adenosyl)-P^5-(5′-thymidyl)pentaphosphate (TP_5A) or P^1-(5′-adenosyl)-P^5-[5′-(3′-azido-3′-deoxythymidine)] pentaphosphate (AZT-P_5A) reported herein provide a structural explanation for our kinetic observations and supply important insights as to how TmpKs achieve catalysis. In addition, this is a structure of what we term a type II TmpK, which differs from type I TmpKs (e.g., yeast and human TmpKs) in their P loop and Lid sequences.

MATERIALS AND METHODS

Synthesis and K_d Determination of TP_5A and AZT-P_5A. AZT-MP was synthesized by incubating AZT with two equivalents of phosphorus oxychloride under conditions of basic catalysis (2,6-dimethylpyridine). The bisubstrate inhibitors TP_5A and AZT-P_5A were prepared by condensation of adenosine tetraphosphate and dTMP or AZT-MP (activated by

The publication costs of this article were defrayed in part by page charge payment. This article must therefore be hereby marked "*advertisement*" in accordance with 18 U.S.C. §1734 solely to indicate this fact.

This paper was submitted directly (Track II) to the *Proceedings* office.

Abbreviations: TP_5A, P^1-(5′-adenosyl)-P^5-(5′-thymidyl)pentaphosphate; AZT-P_5A, P^1-(5′-adenosyl)-P^5-[5′-(3′-azido-3′-deoxythymidine)]pentaphosphate; AZT, 3′-azido-3′-deoxythymidine; AZT-MP, AZT 5′-monophosphate; TmpK, thymidylate kinase; GAP, GTPase-activating protein.

Data deposition: The atomic coordinates have been deposited in the Protein Data Bank, Biology Department, Brookhaven National Laboratory, Upton, NY 11973 (PDB ID codes 4TMK for TP5A1 and 5TMP for AZTP5A).

†N.O. and R.B. contributed equally to this work.

§To whom reprint requests should be addressed. e-mail: ilme.schlichting@mpi-dortmund.mpg.de.

diphenyl phosphorochloridate) as described (11) for the synthesis of AP_5A.

The fluorescent TP_5A analog TP_5A-MANT [the fluorescent *N*-methylanthraniloyl (MANT) group is on the ribose of the adenosine moiety] was prepared as described (12) for the preparation of MANT-AP_5A. Fluorescence measurements were performed with a SLM 8100 spectrofluorimeter as described (12) with an excitation wavelength of 360 nm and an emission wavelength of 440 nm. The experiments were carried out at 25°C in a buffer containing 100 mM Tris·HCl (pH 7.5), 5 mM $MgCl_2$, 2 mM EDTA, and 100 mM KCl.

Protein Preparation and Crystallographic Analysis. *E. coli* TmpK was cloned from genomic DNA into a pJC20 vector, expressed in *E. coli* BL21(DE3), and purified to homogeneity as described (10). Crystals of the complex of *E. coli* TmpK with either TP_5A or AZT-P_5A were grown by the vapor diffusion method using the hanging drop geometry. An enzyme solution (15 mg/ml) was premixed with the nucleotide solution to contain (final concentrations) enzyme (12 mg/ml) and 2 mM nucleotide. Typically, 4 μl of the enzyme/nucleotide mixture was mixed with 2 μl of a solution containing 1.25 M ammonium phosphate (pH 8.0) and left to equilibrate at 20°C against a reservoir of 2.5 M ammonium phosphate. Crystals with typical dimensions of 500 × 400 × 100 μm grew after a few days in space group *R*32. Molecular replacement with the yeast TmpK model was not successful. For heavy-atom soaking trials, the crystals were transferred to a solution of 1.6 M sodium/potassium tartrate and 100 mM Tris·HCl (pH 8.0). This resulted in a doubling of the *c* axis cell length and in a dimer instead of a monomer in the asymmetric unit. Heavy-atom screening was done by soaking the crystals overnight in a tartrate solution containing 1 mM of the heavy atom being analyzed before mounting in quartz capillaries. X-ray data were collected at 4°C by using a Siemens Hi-Star area detector mounted on a Mac Science rotating anode generator operated at 45 kV and 100 mA. Data were processed with XDS (13) and merged with XSCALE. Only crystals soaked with ethylmercury phosphate were isomorphous with the native crystals, with two mercury atoms bound per monomer. Refinement of heavy-atom positions with MLPHARE (14) followed by phase improvement through 2-fold noncrystallographic symmetry averaging, solvent flattening, and histogram matching with the program DM (15), resulted in an easily interpretable electron-density map. Model building was done with the program O (16). The $TmpK_{yeast}$ model was moved as a rigid body into the density, a procedure that required readjusting the relative positions of the secondary structural elements. Rigid-body refinement followed by simulated annealing and B group refinement to 2.4-Å resolution with X-PLOR (17) resulted in a model with R_{work} = 24% and R_{free} = 29%. Further refinement including bulk solvent correction and individual B factor refinement was done with a data set collected at the Max-Planck beam line BW6 (DESY) of a frozen crystal with a monomer in the asymmetric unit. Crystals of $TmpK_{coli}$ complexed with AZT-P_5A were grown under conditions similar to those used for TP_5A. X-ray data were measured from a single crystal at 4°C by using a Siemens Hi-Star area detector, reduced with XDS and merged with XSCALE. The complex with AZT-P_5A is isomorphous to that with TP_5A, so the refinement was started with the *E. coli* TmpK–TP_5A model. Refinement statistics are shown in Table 1.

RESULTS AND DISCUSSION

Overall Structure. The crystal structures of *E. coli* TmpK (213 amino acid residues) complexed with the bisubstrate inhibitors TP_5A or AZT-P_5A were solved at 2.0-Å and 2.2-Å resolution, respectively. In comparison to the previously determined yeast TmpK (29% amino acid identity), the bacterial enzyme has a similar α/β fold that consists of nine α-helices that surround a five-stranded β-sheet core and is likewise a homodimer. Overlaying the yeast TmpK model with the *E. coli* TmpK model results in good overlap of the β-sheet core (rms deviation for five strands, 27 Cα atoms, 0.36 Å) but the surrounding helices have moved relative to each other (rms deviation for nine helices, 113 Cα atoms, 2.88 Å). This explains the failure of the molecular replacement attempt and the need for the *de novo* structure determination.

NMP kinases and many other nucleotide binding proteins contain a sequence motif (GX_4GKS/T), called the P loop, whose function is to bind nucleoside di- or triphosphates (18). NMP kinases bind an additional nucleotide substrate, a NMP, and catalyze the reversible phosphoryl transfer from the triphosphate [preferably ATP for TmpKs (19)] to the monophosphate (dTMP). In all previously determined NMP kinase structures, the monophosphate is bound in a deep cleft with the nucleobase surrounded by protein residues. The triphosphate is bound (mainly by the P loop) with its phosphates facing that of the monophosphate and is observed to interact with a region called Lid. The closure of the Lid region upon triphosphate binding acts in most NMP kinases to bring catalytic arginines to the reaction center. $TmpK_{yeast}$ was the first NMP kinase observed to deviate from this principle; although there is a Lid region near the triphosphate, it lacks positively charged catalytic residues. In contrast, $TmpK_{coli}$ does possess positively charged residues in its Lid region that are observed to interact with ATP. On the basis of this difference between $TmpK_{coli}$ and $TmpK_{yeast}$, we have categorized TmpKs in to two types. Type I TmpKs (e.g., yeast and human) have a basic residue in their P loop sequence (in addition to the invariant lysine) that can interact with the γ-phosphate of ATP and lack such residues in the Lid region. The situation is reversed for type II TmpKs (e.g., *E. coli*), which are thus more similar to other NMP kinases, such as adenylate kinase or uridylate kinase, that have a glycine in the P loop and basic residues in the Lid region that interact with ATP.

A unique feature of TmpKs of both types is that a residue in the P loop (Asp-14 in $TmpK_{yeast}$ and Glu-12 in $TmpK_{coli}$) interacts with the nucleotide monophosphate via hydrogen bond(s) with the 3′-hydroxyl of the deoxyribose. This interaction has far reaching implications for ribose modification.

Nucleotide Binding. The bisubstrate inhibitors TP_5A and AZT-P_5A are bound tightly to the enzyme (K_d values of 20 nM and 34 nM, respectively) in accordance with their relatively low B factors. A distance map showing the interactions between TP_5A and $TmpK_{coli}$ is shown in Fig. 1*a*. The complex was crystallized at high phosphate concentration, which is not compatible with the presence of free magnesium. Attempts to soak in magnesium after crystal transfer to ammonium sulfate or potassium tartrate solutions resulted in the loss of high-resolution diffraction.

Many of the interactions between the nucleotide and $TmpK_{coli}$ are similar to those in $TmpK_{yeast}$. For dTMP binding, conserved interactions are the base-stacking interaction of the thymidine base with a phenylalanine (Phe-74), a H-bond between the O4 carbonyl and an arginine side chain (Arg-78), and the use of a tyrosine residue (Tyr-108) to discriminate against ribonucleotides. Although in the yeast enzyme the base makes further interactions with tightly bound water molecules, the *E. coli* enzyme uses the side chains of Thr-105 and Gln-109. The most striking difference is the interaction of the 3′-hydroxyl with the P loop carboxylic acid (Fig. 1*b*): this is a bidentate interaction in the yeast enzyme (Asp-14), but a side-on interaction in the *E. coli* enzyme (Glu-12). The adenine base and phosphate interactions are also very similar in the two TmpKs. The Lid region of $TmpK_{coli}$ contains the highly basic amino acid sequence ^{148}KRARAR^{153} but only Arg-153 interacts with the phosphates. Arg-149 stacks against the adenine base and Arg-151 points toward the solvent.

Table 1. Data collection, phasing, and refinement statistics

	TP_5A1	TP_5A2	EMP	AZT-P_5A
Data collection statistics				
Temperature, K	100	277	277	277
Resolution, Å	2.0	2.2	2.8	2.2
Wavelength, Å	1.07	1.54	1.54	1.54
Observed reflections, no.	117,407	127,088	89,490	56,386
Unique reflections, no.	21,854	36,046	17,427	15,949
Completeness, % (overall/last shell)	95.5/95.9	98.0/86.8	96.9/84.4	90.4/80.0
R_{sym}[1], % (overall/last shell)	4.5/13.6	7.4/39.3	8.3/23.1	6.5/24.8
Space group	*R*32	*R*32	*R*32	*R*32
Unit cell, Å				
a, *b*	151.7	151.4	151.4	152.1
c	74.5	164.0	163.9	75.6
Molecules/asymmetric unit, no.	1	2	2	1
Phasing statistics				
Heavy atom sites, no.			4	
R_{iso}[2]			0.16	
R_{Cullis}[3]			0.66	
Phasing power[4]			1.6	
Mean figure of merit after MLPHARE			0.43	
Refinement statistics				
R_{cryst}[5], %	20.4			20.9
R_{free}[6], %	25.3			27.0
Resolution range, Å	19.4–2.0			15.0–2.2
Reflections with $\mathbf{F} > 0\ \sigma$ (working/test)	20,773/1,067			13,854/717
No. protein/water/nucleotide atoms	1,662[7]/168/60[8]			1,679[9]/72/72[10]
rms deviations				
Bond lengths, Å	0.013			0.011
Bond angles, degrees	1.620			1.487
Dihedral angles, degrees	22.63			23.30
Improper angles, degrees	1.159			1.535
Average *B*, Å^2				
Main chain	22.7			28.4
Side chain	25.3			31.5
Water molecules	33.4			33.6
Nucleotides	21.2			30.1

EMP, ethylmercury phosphate.

[1] $R_{sym} = \Sigma\ |I_{obs} - \langle I\rangle|/\Sigma\ \langle I\rangle$.

[2] $R_{iso} = \Sigma\ |\mathbf{F}_{ph} - \mathbf{F}_p|/\Sigma\ \mathbf{F}_p$, summed over all unique reflections.

[3] $R_{Cullis} = \Sigma\ \|\mathbf{F}_{ph,obs} - \mathbf{F}_{p,obs}| - \mathbf{F}_{h,calc}|/\Sigma\ |\mathbf{F}_{ph,obs} - \mathbf{F}_{p,obs}|$.

[4] Phasing power $= \Sigma\ |\mathbf{F}_h|/\Sigma\ \|\mathbf{F}_{ph,obs}| - |\mathbf{F}_{ph,calc}\|$.

[5] $R_{cryst} = \Sigma|\mathbf{F}_{obs} - \mathbf{F}_{calc}|/\Sigma\ \mathbf{F}_{obs}$.

[6] $R_{free} = R_{cryst}$, calculated for 5% randomly selected reflections not included in the refinement.

[7] Number includes atoms due to double conformations in residues Arg-51 and Gln-180. Met-1 was not modeled, and Arg-2 and His-118 were modeled as alanine.

[8] Number includes five atoms in alternate conformations.

[9] Number includes atoms due to double conformations in residues Arg-33 and Phe-164. Met-1 was not modeled, and Arg-2 and Lys-182 were modeled as alanine.

[10] Number includes 15 atoms in alternate conformations.

Unlike the TP_5A–$TmpK_{yeast}$ complex (10), where the phosphates are observed in only one conformation, in the TP_5A–$TmpK_{coli}$ complex, the middle phosphate is observed in two conformations, and in the AZT–P_5A-$TmpK_{coli}$ complex, four phosphates were modeled with alternate conformations. The phenomenon of multiple conformations has also been observed in a complex of adenylate kinase and AP_5A (20). This may be a consequence of the interaction of the phosphates with an arginine of the Lid region and a consequence of the absence of magnesium, which would stabilize one conformation but not the other.

The comparison between the $TmpK_{coli}$ complex with TP_5A and that with AZT-P_5A shows a nearly identical protein structure (rms deviation of 0.23 Å on 208 Cα atoms). However, three differences between the structures are significant. The first is a rotation of the deoxyribose moiety of thymidine and of three carboxylic acid side chains located in close proximity to the 3′ position. The rotation of the whole deoxyribose as a rigid body around the C1′ and C4′ atoms can be attributed to the azido group that would otherwise be too close to the side chain of Glu-12 (Fig. 1*d*). Concomitantly, Glu-12 rotates in the opposite direction to make space for the azido group. In addition, the rigid body rotation of the deoxyribose forces Glu-160 to adjust its position. The side chains of Glu-12 and Asp-157 are only 2.6 Å apart in the TP_5A complex structure (3.1 Å in the AZT-P_5A complex), suggesting that the pK_a of these acids is perturbed and that at least one of them is protonated at physiological pH. The second difference between the structures is the conformation of the phosphates of the bound TP_5A and AZT-P_5A, which could be attributed to the rigid-body rotation of the deoxyribose forced upon by the azido group. However, this did not change the positions of the nucleobases. The third important difference between the complexes is a slight change at the tip of the P loop, probably caused by the different phosphate conformations, as it is the P loop that interacts the most with the phosphates.

Structural Explanation for Fast AZT-MP Phosphorylation. The crystal structure of $TmpK_{yeast}$ complexed with TP_5A (10)

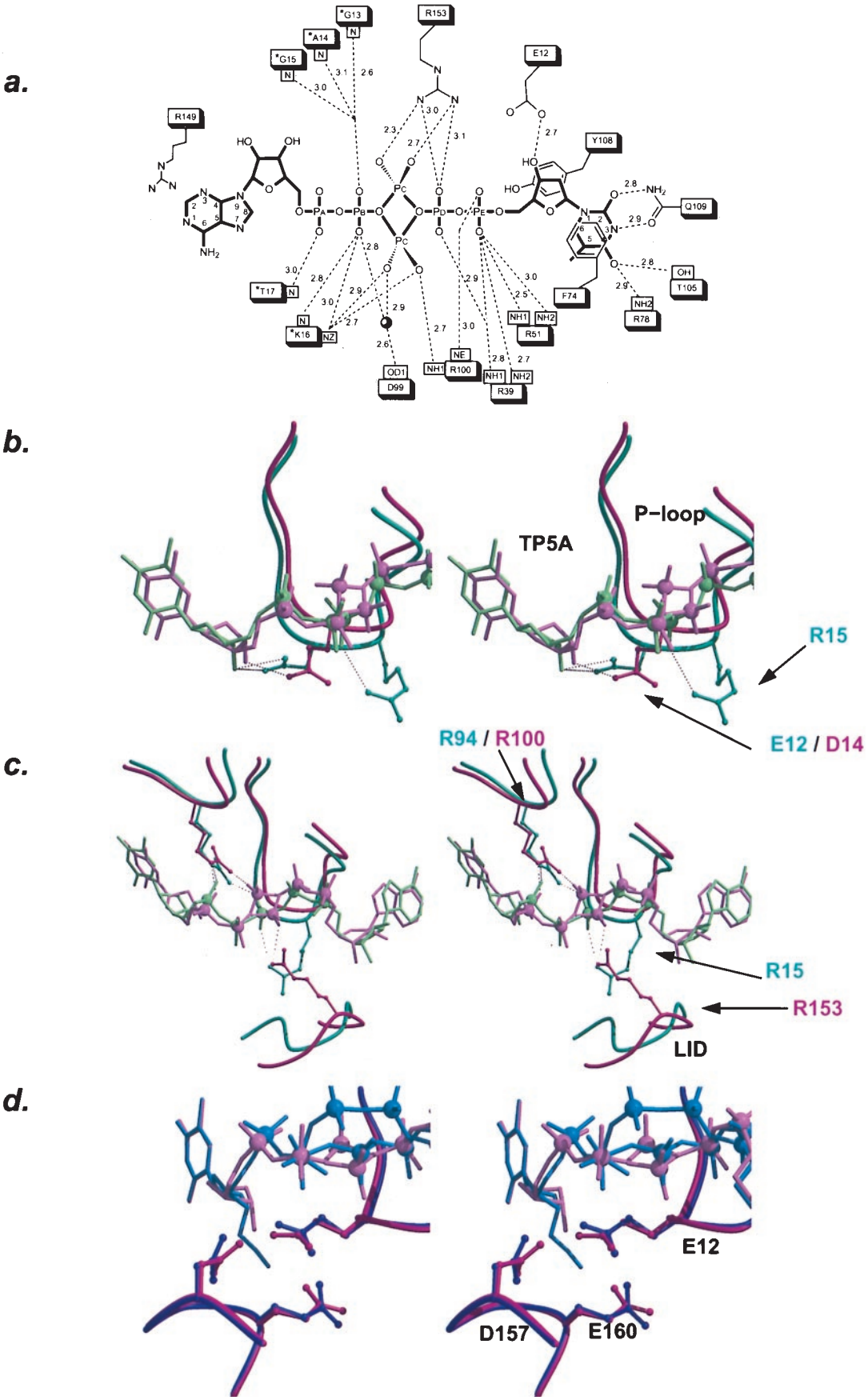

FIG. 1. Interactions of the bisubstrate inhibitor with TmpK (*a*). Distance map of TP_5A bound to $TmpK_{coli}$. P loop residues are marked with an asterisk. (*b–d*) Stereoviews. Overlay of the $TmpK_{coli}$–TP_5A complex model (pink) with the $TmpK_{yeast}$–TP_5A model (green) (*b* and *c*) or the $TmpK_{coli}$–$AZTP_5A$ (blue) (*d*). (*b*) Interactions of the 3′-hydroxyl of the thymidine deoxyribose. In $TmpK_{yeast}$, a bidentate interaction between the P loop aspartic acid and the sugar hydroxyl is observed. The binding of AZT-MP causes the P loop to move, thus displacing the catalytic P

suggests that the arginine situated in the P loop sequence is used to stabilize the transition state (in addition to other basic residues). The P loop of *E. coli* has a glycine at this position. Although the yeast enzyme has only one basic residue in the Lid region that does not interact with the phosphate groups, the bacterial enzyme has four basic residues in its Lid region (Fig. 2). Therefore, we postulated that an arginine from the *E. coli* Lid region fulfills a similar role to that of the arginine in the P loop of the yeast enzyme (10). The structural overlay of the yeast and *E. coli* TmpKs confirms our hypothesis. The tip of Arg-15 (yeast), which interacts with the middle phosphate of TP_5A, is spatially very close to the tip of Arg-153 (*E. coli*), which also interacts with the middle phosphate (Fig. 1*c*).

This observation may in part explain the kinetic differences observed between the two TmpKs (i.e., $TmpK_{yeast}$ and $TmpK_{coli}$) with respect to their AZT-MP phosphorylation rates. For $TmpK_{yeast}$, the binding of AZT-MP induces some movement of the P loop via the interaction of the P loop aspartic acid with the 3′-azido group. This movement of the P loop results in a reduced catalytic rate that can be attributed to at least three factors. The P loop has the function of binding the phosphoryl donor, in this case ATP, so any relative shift of the positions of the two substrates could decrease the catalytic rate. A further reason could be the movement of the P loop arginine, which presumably fulfills a catalytic role. Lastly, the shift of the aspartic acid (Asp-14 in yeast), an essential residue for catalysis (unpublished results), could also account for the reduced rate. It cannot be ruled out that it is a combination of the above three reasons that leads to the reduction of catalytic activity.

In contrast, on comparing the complexes of $TmpK_{coli}$ with TP_5A and with AZT-P_5A, no significant P loop movement is seen. The small adjustment that is required for fitting the bulkier azido group seems to be restricted to a slight rotation of the whole 3′-azido-deoxyribose moiety and the side chain of the P loop glutamate. Because the interaction of the P-loop carboxylic acid with the 3′ group is side-on, unlike the bidentate interaction seen in $TmpK_{yeast}$, the side chain can adjust relatively easily to AZT-MP binding. In addition, because in $TmpK_{coli}$ a presumed catalytic arginine originates from the Lid region, any P loop perturbation should not effect that residue. These are the structural reasons why the rate of AZT-MP phosphorylation is only 2-fold slower than that of dTMP.

Role of Arginines in Phosphoryl Transfer Reactions. The use of arginines from the Lid region in $TmpK_{coli}$ would be in analogy to other NMP kinases such as adenylate kinase (21) or uridylate kinase (22, 23) that use basic residues from the Lid region for transition state stabilization. $TmpK_{yeast}$ lacks such basic Lid residues and uses its P loop arginine instead. Thus, two types of TmpKs have evolved; type I, which stabilize the negative charge in the transition state by having the positively charged guanidinium group originating from the P loop (i.e., yeast enzyme), and type II, where the guanidinium group originates from the Lid region (*E. coli* enzyme).

A similar situation is encountered when comparing two types of GTPases, the heterotrimeric G proteins and GTPases belonging to the Ras superfamily. In the former, a catalytically essential arginine is present in the G_α subunits. These subunits are made up of two domains—one is the Ras-like GTP-binding domain and the other is an α-helical domain. An arginine residue positioned by the α-helical domain (residue 178 in $G_{i\alpha}$)

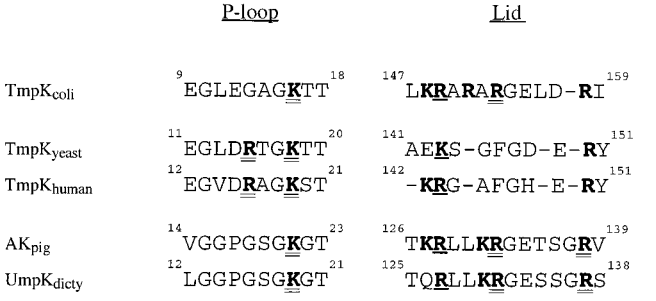

FIG. 2. Structure-based sequence alignment of the P loop and Lid regions. Lysine and arginine residues that make phosphate interactions are underlined doubly and those that make a stacking interaction with the adenine base are underlined singly. TmpKs are unique in having a carboxylic acid situated at the tip of the P loop (Glu-12 in $TmpK_{coli}$). In type I TmpKs (e.g., human and yeast), the following residue is an arginine that has been shown to be catalytically important for the yeast enzyme. Type II TmpKs (e.g., *E. coli*) lack this arginine, having instead a number of basic residues in their Lid region: for $TmpK_{coli}$, Arg-153 presumably fulfills a catalytically role analogous to that of Arg-15 in yeast. Although the last Lid arginine in TmpKs (Arg-158 in $TmpK_{coli}$) aligns well with catalytic arginines from pig adenylate kinase (AK_{pig}) and *Dictyostelium* uridylate kinase ($UmpK_{dicty}$), it points away from the active site, thus having no obvious catalytic role. The eukaryotic TmpKs have no catalytic residues in the Lid region.

is involved in stabilizing the transition state (24). Ras and Ras-like proteins do not have an equivalent arginine residue and are consequently much slower GTPases than the G_α subunit. However, such a residue can be supplied by GTPase-activating proteins (GAPs), turning them into efficient GTP-hydrolyzing enzymes. Comparing the structure of the $G_{i\alpha}$ transition state analog complex (24) with those of similar complexes such as Ras–RasGAP (25) or Rho–RhoGAP (26) shows that the catalytic arginine, while fulfilling the role of stabilizing the transition state by interaction with the γ-phosphate, approaches this phosphate from quite different directions. Thus, in GTPases and kinases, catalysis by arginine can occur as long as the interaction with the transferred phosphate group is possible, regardless of where the arginine is located in the secondary structure. We can now identify four different situations for catalytic arginines in phosphate-transferring enzymes; the arginine can be located in the P loop ($TmpK_{yeast}$), in another region (Lid region of a single domain protein such as $TmpK_{coli}$ and various other NMP kinases), in a different domain of a multidomain protein (heterotrimeric G proteins), or in another protein capable of interacting with the phosphate-transferring protein (Ras–RasGAP). Interestingly, there are differences in the details of the interactions, as can be seen best by comparing the transition-state analog complex structures of $G_{i\alpha}$ (24), Ras–RasGAP (25), Rho–RhoGAP (26), and uridylate kinase (22). Arginine side chains, because they possess three basic nitrogens, can form the appropriate interaction from a variety of spatial situations.

In NMP kinases there is an additional arginine located neither in the P loop nor the Lid region that appears to play an important role. This is residue 100 in $TmpK_{coli}$ (94 in $TmpK_{yeast}$), and it appears to be conserved in structural space in other members of the family (Fig. 1*c*). In all cases examined so far, this residue appears to concomitantly interact with both the γ-phosphate of ATP and the phosphate of the nucleoside

loop arginine. In contrast, in $TmpK_{coli}$, the interaction between Glu-12 and the 3′-hydroxyl is side-on, and the bulkier azido group does not induce a significant movement of the P loop. (*c*) Similar phosphate–arginine interactions made in $TmpK_{yeast}$ by Arg-15 and in $TmpK_{coli}$ by Arg-153. Displayed are the P loop and a part of the Lid region. The structures were overlaid according to the position of the bisubstrate inhibitor. (*d*) In the $TmpK_{coli}$–TP_5A and the $TmpK_{coli}$–$AZTP_5A$ complex structures, the thymine base is at an identical position, but the deoxyribose moiety has undergone a rigid-body rotation caused by the azido group in the AZT-P_5A complex. In addition, Glu-12 has rotated slightly to provide more room for the azido group. The rotation of the deoxyribose induces a similar rotation of the Glu-160 side chain. As Glu-12 makes close interactions with Asp-157, the latter carboxylic acid also rotates slightly. *b–d* were generated by using BOBSCRIPT (29, 30) and RASTER 3D (31).

monophosphate (i.e., the transferred phosphate and the acceptor phosphate). The interactions are with different nitrogens of the arginine side chain, and the possible significance of this is that such a two pronged interaction could act like a vice or clamp, pulling the charged phosphate groups toward each other while partially neutralizing their repulsive negative charges. However, among the various NMP kinases, this type of interaction only seems to be crucial for TmpK because mutagenesis studies have indicated that this residue is not essential for adenylate kinase activity (27, 28). A possible explanation for this difference is that TmpKs uses three basic residues to interact with the transferred phosphoryl group, whereas adenylate kinase or uridylate kinase use five.

Conclusion. We have shown herein that the capability of the *E. coli* P loop glutamic acid to accommodate AZT-MP without major structural changes in comparison to dTMP, the lack of a catalytic arginine in the P loop, and the presence of a presumably catalytic arginine in the Lid region are the structural reasons for the efficient phosphorylation of AZT-MP by $TmpK_{coli}$. The endeavor to use this newly acquired understanding for the purpose of modifying the human TmpK so that the AZT-MP phosphorylation rate is increased is presently underway.

We thank Georg Holtermann and Sonja Hönig for skilled technical assistance and Gleb Bourenkov for help in data collection. A.L. was supported by the Peter and Traudl Engelhorn Stiftung (Germany).

1. Bridges, E. G., Faraj, A. & Sommadossi, J. P. (1993) *Biochem. Pharmacol.* **45,** 1571–1576.
2. Harrington, J. A., Reardon, J. E. & Spector, T. (1993) *Antimicrob. Agents Chemother.* **37,** 918–920.
3. Yan, J. P., Ilsley, D. D., Frohlick, C., Steet, R., Hall, E. T., Kuchta, R. D. & Melancon, P. (1995) *J. Biol. Chem.* **270,** 22836–22841.
4. Frick, L. W., Nelson, D. J., St. Clair, M. H., Furman, P. A. & Krenitsky, T. A. (1988) *Biochem. Biophys. Res. Commun.* **154,** 124–129.
5. Fridland, A., Connelly, M. C. & Ashmun, R. (1990) *Mol. Pharmacol.* **37,** 665–670.
6. Elion, G. B., Furman, P. A., Fyfe, J. A., de Miranda, P., Beauchamp, L. & Schaeffer, H. J. (1977) *Proc. Natl. Acad. Sci. USA* **74,** 5716–5720.
7. Guettari, N., Loubiere, L., Brisson, E. & Klatzmann, D. (1997) *Virology* **235,** 398–405.
8. Lavie, A., Vetter, I. R., Konrad, M., Goody, R. S., Reinstein, J. & Schlichting, I. (1997) *Nat. Struct. Biol.* **4,** 601–604.
9. Lavie, A., Schlichting, I., Vetter, I. R., Konrad, M., Reinstein, J. & Goody, R. S. (1997) *Nat. Med.* **3,** 922–924.
10. Lavie, A., Konrad, M., Brundiers, R., Goody, R. S., Schlichting, I. & Reinstein, J. (1998) *Biochemistry* **37,** 3677–3686.
11. Feldhaus, P., Fröhlich, T., Goody, R. S., Isakov, M. & Schirmer, R. H. (1975) *Eur. J. Biochem.* **57,** 197–204.
12. Reinstein, J., Vetter, I. R., Schlichting, I., Rösch, P., Wittinghofer, A. & Goody, R. S. (1990) *Biochemistry* **29,** 7440–7450.
13. Kabsch, W. (1993) *J. Appl. Cryst.* **24,** 795–800.
14. Otwinowski, Z. (1991) in *Maximum Likelihood Refinement of Heavy Atom Parameters*, eds. Wolf, W., Evans, P. R. & Leslie, A. G. W. (SERC Daresbury Laboratory, Warrington, U.K.).
15. Cowtan, K. (1994) *Joint CCP 4 and ESF-EACBM Newsletter on Protein Crystallography* **31,** 24–28.
16. Jones, T. A., Zhou, J.-Y., Cowan, S. W. & Kjeldgaard, M. (1991) *Acta. Cryst. A* **47,** 110–119.
17. Brünger, A. T. (1993) X-PLOR, A System for X-Ray Crystallography and NMR (Yale Univ. Press, New Haven, CT).
18. Saraste, M., Sibbald, P. R. & Wittinghofer, A. (1990) *Trends Biochem. Sci.* **15,** 430–434.
19. Jong, A. Y. & Campbell, J. L. (1984) *J. Biol. Chem.* **259,** 14394–14398.
20. Müller, C. W. & Schulz, G. E. (1992) *J. Mol. Biol.* **224,** 159–177.
21. Berry, M. B., Meador, B., Bilderback, T., Liang, P., Glaser, M. & Phillips, G. N., Jr. (1994) *Proteins* **19,** 183–198.
22. Schlichting, I. & Reinstein, J. (1997) *Biochemistry* **36,** 9290–9296.
23. Scheffzek, K., Kliche, W., Wiesmüller, L. & Reinstein, J. (1996) *Biochemistry* **35,** 9716–9727.
24. Coleman, D. E., Berghuis, A. M., Lee, E., Linder, M. E., Gilman, A. G. & Sprang, S. R. (1994) *Science* **265,** 1405–1412.
25. Scheffzek, K., Ahmadian, M. R., Kabsch, W., Wiesmuller, L., Lautwein, A., Schmitz, F. & Wittinghofer, A. (1997) *Science* **277,** 333–338.
26. Rittinger, K., Walker, P. A., Eccleston, J. F., Smerdon, S. J. & Gamblin, S. J. (1997) *Nature (London)* **389,** 758–762.
27. Reinstein, J., Gilles, A. M., Rose, T., Wittinghofer, A., Saint Girons, I., Barzu, O., Surewicz, W. K. & Mantsch, H. H. (1989) *J. Biol. Chem.* **264,** 8107–8112.
28. Dahnke, T., Shi, Z., Yan, H., Jiang, R. T. & Tsai, M. D. (1992) *Biochemistry* **31,** 6318–6328.
29. Esnouf, R. (1997) *J. Mol. Graphics* **15,** 133–138.
30. Kraulis, P. J. (1991) *J. Appl. Crystallogr.* **24,** 946–950.
31. Merrit, E. A. & Murphy, M. E. P. (1994) *Acta Crystallogr. D* **50,** 869–873.